ASTRO-H

INSTRUMENT CALIBRATION REPORT
SXS BLOCKING FILTER TRANSMISSION
ASTH-SXS-CALDB-BLCKFILT

Version 1.0

DATE December 19th 2016

ISAS/ GSFC

Prepared by: Maurice Leutenegger, Megan Eckart, Greg Brown(LLNL)

Table of Contents

.

CHANGE RECORD PAGE (1 of 2)

DOCUMENT TITLE : SXS BLOCKING FILTER TRANSMISSION			
ISSUE	DATE	PAGES AFFECTED	DESCRIPTION
Version 1.0	December 19 2016	All	First release

Introduction

1.1 Purpose

This document describes the measurement and calculation of the X-ray transmission of the SXS dewar internal optical/thermal blocking filters.

1.2 Scientific Impact

The effective area of the SXS instrument includes the transmission of the filters. Note that because of the loss of the mission before the SXS beryllium gate valve was opened, the detailed modeling of the filter transmission below 2 keV will not be relevant to astronomical data analysis.

2 Release CALDB 20160310

Filename	Valid data	Release data	CALDB Vrs	Comments
ah_sxs_blckfilt_20140101v001.fits	2014-01-01	20160310	001	From file FM_stack_model_0.2.2.fits

2.1 Data Description

The SXS optical/thermal blocking filters consist of five filters internal to the SXS dewar, all of which attenuate X-rays propagating from the telescope to the calorimeter array. The two innermost filters, the CTS and DA filters, consist of thin aluminized polyimide (Al/PI) films mounted freestanding on backing rings. The three outermost filters, the IVCS, OVCS, and DMS filters, consist of thin aluminized polyimide (Al/PI) films mounted on silicon meshes with epoxy. The silicon meshes consist of a coarse mesh with thick bars and large cell size, and a fine mesh with thin bars and small cell size. The thin films are mounted to the fine mesh. The filter design and specifications are discussed in more detail in Kilbourne et al. (2016).

The filter transmission is calculated primarily based on measurements made at the NSLS and CLS synchrotrons. NSLS data constrain the broadband filter transmission, fine support mesh filling fraction, epoxy filling fraction and thickness, and photoelectric absorption edge structure. CLS data were used to improve the quality of the photoelectric absorption edge structure measurements. The coarse mesh filling fraction is derived from photographic measurements of mesh dimensions.

The NSLS measurements were carried out at two beamlines, U3C and X8A. The U3C measurements used a reflection grating monochromator over the energy range 250-1000 eV. The X8A measurements used a multilayer monochromator over the range 1000-2100 eV and a Si 111

Bragg crystal monochromator over the range 2100-6000 eV. For each filter we used the two beamlines to coarsely sample the transmission on at least a 50 eV interval over the range 260-2100 eV. We also measured the edge structure at the C, N, and O K edges. We did not measure the structure of the Al K edge at high resolution at NSLS.

Transmission measurements on mesh-mounted filters were performed using an aperture large enough to average over the fine mesh, but small enough to center the beam inside of a hole in the coarse mesh without hitting the coarse mesh bars.

We also measured transmissions for "stacks" of five filters, allowing us to check for systematic errors in individual filter measurements. These stack measurements were used as data validation checks.

At CLS, we used the STXM beamline, equipped with grating monochromators and a zone plate to focus light on the sample, to measure the Al K edge structure of witness samples of aluminized polyimide made from the same lots as the SXS flight filters. We also obtained further measurements of the C, N, and O K edges at higher resolution than the NSLS measurements.

2.2 Data Analysis

The NSLS data were analyzed as follows. Each measurement consists of a series of diode current readings from a pair of Si diodes, with one fixed permanently behind the sample ("detector"), and one that can be inserted intermittently into the beam in front of the filter ("monitor"). The differences in QE of the diodes as a function of beam energy are calibrated by performing the same measurements in the absence of a filter. For each energy point, the transmission is thus given by $T(E) = (I_d / I_m) * (I_{m0} / I_{d0})$, where the subscripts "d" and "m" refer to the detector and monitor, respectively, and the subscript "0" refers to measurements in the absence of a sample.

The broadband transmission curve measured for each filter using the two beamlines is fit with a model in which the free parameters are polyimide thickness, aluminum thickness, oxide thickness; and for mesh-mounted filters only, fine mesh filling fraction, epoxy filling fraction, and epoxy thickness. The fine mesh thickness is fixed to the specified value (8±0.5 μm for the DMS filter, 25±0.5 μm for the IVCS and OVCS filters).

The absorption cross sections are taken from Henke et al. 1993. The epoxy model assumes a distribution of thicknesses ranging between zero and the maximum value specified in the model. The differential distribution of thicknesses is chosen to be quadratic in thickness, and the normalization is set by requiring that the integrated distribution have the same total filling fraction as the corresponding model parameter. The epoxy was modeled as having the same composition as polyimide.

The CLS data were analyzed as follows. The measurements were made on witness samples mounted on small grids, and each sample had a hole poked through part of it. For each energy point, a spatial scan was performed, with part of the scan going through the film, and part going

through the hole. Spatial regions were constructed for each run for sample and hole, and in each region the mean detector current was averaged and normalized for the region size. The transmission was then given by the sample current divided by the current measured in the open hole region.

For the C, N, and O K edges, each edge was fit with an empirical model consisting of a background pre-edge opacity, plus a sum of Gaussian-arctan components. The aluminum edge was not modeled; the data were used to directly interpolate the edge structure in the opacity.

The mesh photographs were analyzed to obtain estimates for the widths of the coarse mesh bars. We calibrated the microscope plate scale using a reticle. We then measured the bar size for each flight filter. We found that the bar width was consistent with the nominal bar width of 65 μm within the measurement error (typically 0.5-1.0 %) for all flight filters. We found that at least one of the flight spare filters was underetched, with a bar width about 5% over the nominal value. The coarse mesh thickness is assumed to be consistent with the specified value of 225±5 μm (IVCS/OVCS) or 208±5 μm (DMS). We neglected the buried oxide layer, which was specified at 0.5 μm ±5%, since it has a small thickness in comparison with the tolerance on the handle layer thickness. These thicknesses were confirmed to be within tolerance by direct measurements of representative meshes.

2.3 Results

The results of our filter calibration campaign are summarized in Eckart et al. (2016), including the best fit parameters for the FM filters, which are given in Tables 1 and 2. Below we show two examples of measured filter transmissions together with best fitting models (Figures 1 and 2). We also show the model transmission for the full stack of five filters (Figures 3 and 4). Note that the CALDB file contains transmission values evaluated on a 0.25 eV grid from 10 eV – 40 keV.

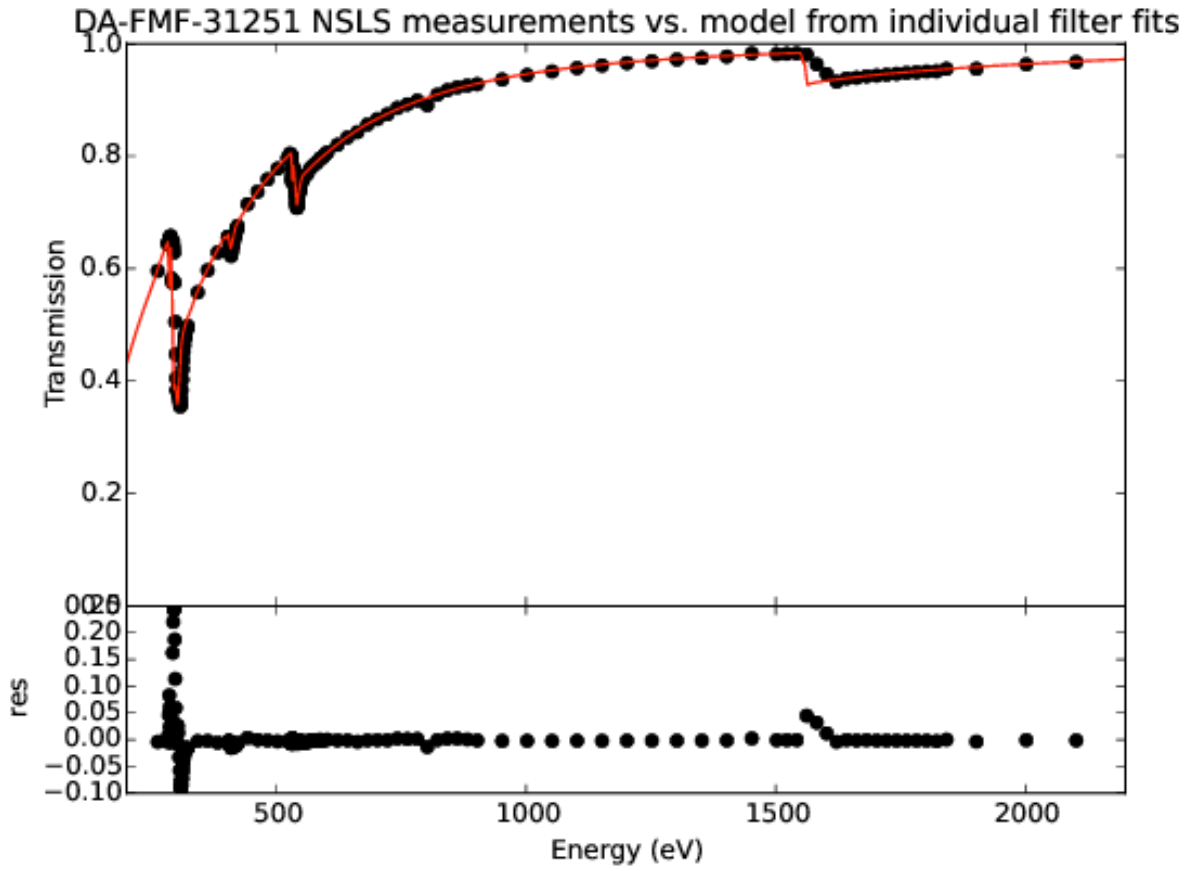

Figure 1. Measured transmission (circles) and model transmission (red line) for filter DA-FMF-31251, which is a pure Al/PI thin film filter with no support mesh. Residuals are shown in the bottom panel. This model does not include a realistic Al K edge, and the multilayer monochromator used at the Al K edge does not resolve the structure. However, the final model used for the FM filter stack does include realistic edges for all important elements. The residuals near the C K edge are due to higher order contamination exacerbated by poor first order transmission caused by carbon compound accumulation on the NSLS beamline optics. These residuals are also present in the CLS scans, but are much weaker; modeling of the C K edge structure was not compromised by these features as they occur at a slightly different energy than the C K edge of polyimide.

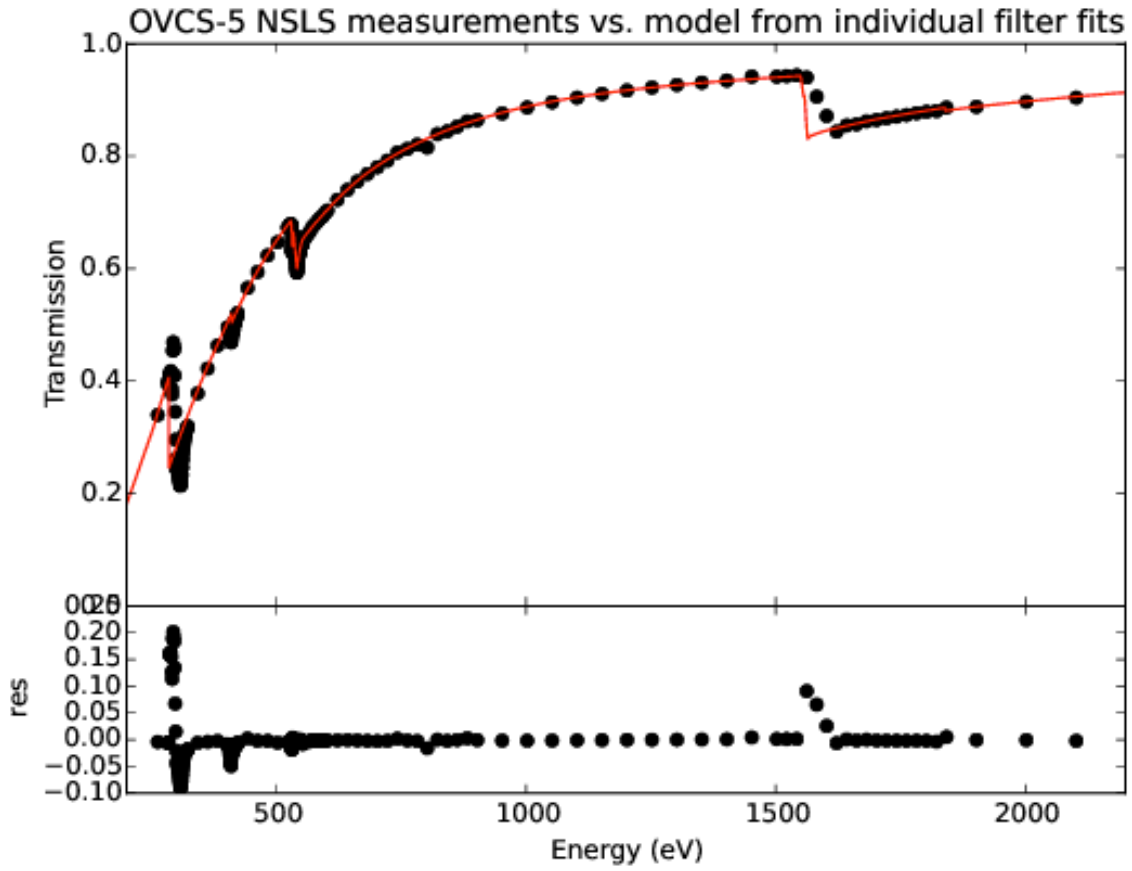

Figure 2. Measured transmission (circles) and model transmission (red line) for filter OVCS-5, which is consists of a thin Al/PI film mounted on a Si mesh. Residuals are shown in the bottom panel. This model does not include a realistic Al K edge, and the multilayer monochromator used at the Al K edge does not resolve the structure. This model also does not include a realistic C K or N K edge. However, the final model used for the FM filter stack does include realistic edges for all important elements. The residuals near the C K edge are mostly due to higher order contamination exacerbated by poor first order transmission caused by carbon compound accumulation on the beamline optics. These residuals are also present in the CLS scans, but are much weaker; modeling of the C K edge structure was not compromised by these features as they occur at a slightly different energy than the C K edge of polyimide.

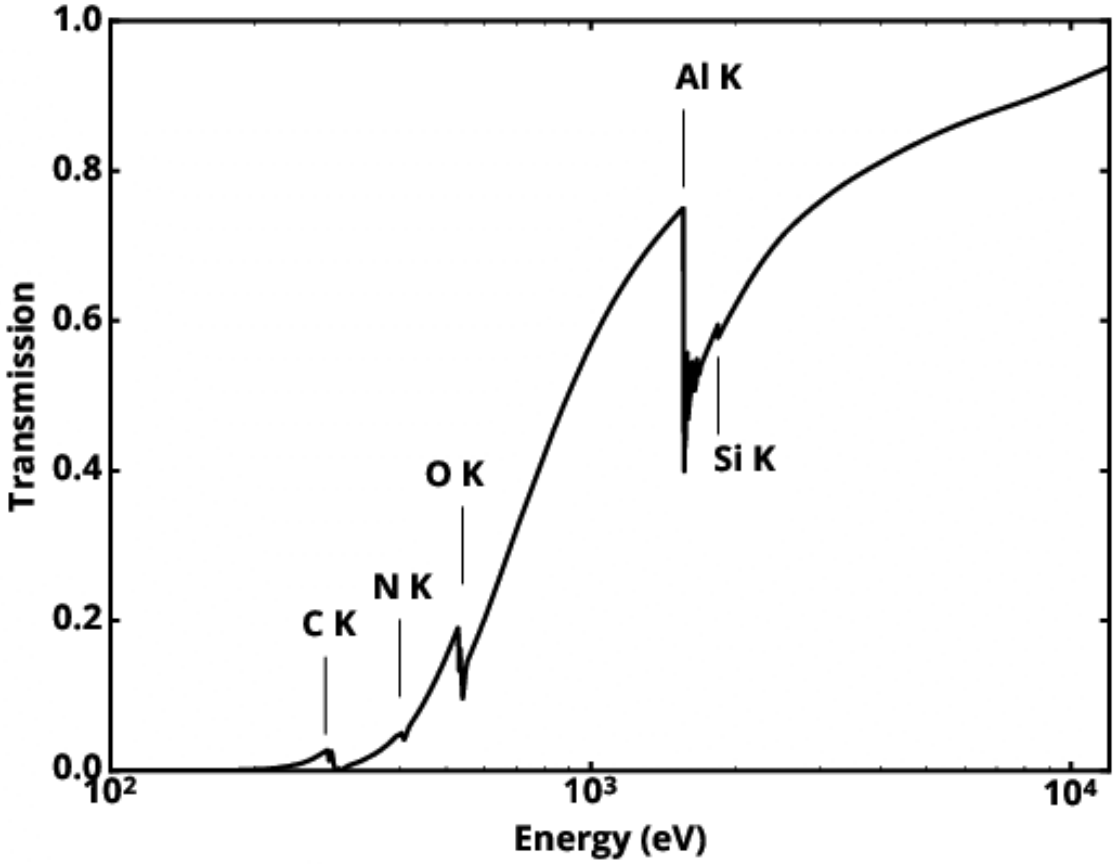

Figure 3. Model transmission for the full filter stack of five FM filters shown over the primary science band pass of the SXS, from 100 eV – 12 keV. Note that the Si K edge shows no structure, since it is nearly saturated. The low depth of the Si K edge is due to the fact that the covering fraction of the fine mesh is small and the silicon is relatively thick (8 or 25 μm).

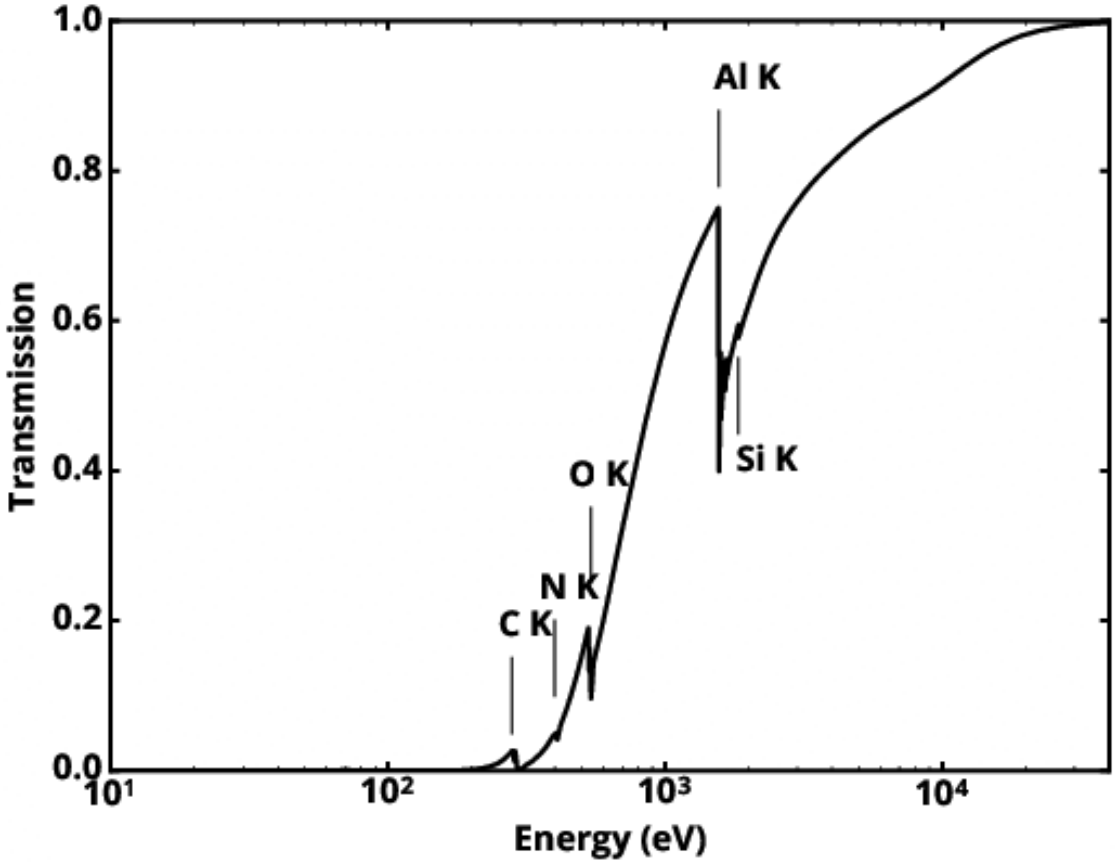

Figure 4. Model transmission for the full filter stack of five FM filters shown over the full range of the CALDB file, from 10 eV – 40 keV.

2.4 Final remarks

This is the first release.

2.5 Bibliography

Eckart et al. 2016 SPIE 9905 3W
"Ground calibration of the Astro-H (Hitomi) soft x-ray spectrometer"

Henke et al. 1993 ADNDT 54 181
"X-ray interactions: photoabsorption, scattering, transmission, and reflection at E=50-30000 eV, Z=1-92"

Kilbourne et al. 2016 SPIE 9905 3Q
"The design, implementation, and performance of the Astro-H SXS aperture assembly and blocking filters"